Pergamon

Cement and Concrete Research, Vol. 28, No. 12, pp. 1687–1693, 1998

0008-8846/98 $–see front matter

PII S0008-8846(98)00153-7

COMMUNICATION

MICROSTRUCTURAL ASPECTS IN A POLYMER-MODIFIED CEMENT

R. Ollitrault-Fichet,* C. Gauthier,† G. Clamen,‡ and P. Boch[1]*

*Ecole Supérieure de Physique et de Chimie Industrielles, 10 rue Vauquelin, 75005 Paris, France

†Matériaux et Structures du Génie Civil, 2 allée Képler, 77420 Champs-sur-Marne, France

‡Rohm & Haas, 371 rue L. V. Beethoven, 06560 Valbonne, France

(Received August 12, 1998; in final form September 4, 1998)

ABSTRACT

Scanning electron microscopic observations of polymer-free and polymer-modified cements have shown that the polymer particles are partitioned between the inside of hydrates and the surface of anhydrous cement grains. Differential thermal analysis, thermogravimetric analysis, and porosimetry experiments show the retardant effect of the polymer and provide information on changes in porosity. © *1998 Elsevier Science Ltd*

Introduction

Polymers can be used for improving mechanical properties, resistance to shrinkage cracking, adhesion with substrate, or waterproof qualities of cement and mortar, particularly for low-thickness parts. Ohama (1) and Chandra and Flodin (2) are among those who have proposed a microstructural model of Portland cement modified by polyacrylic polymer additions. Two main points are 1) a polymer network that embeds the cement grain and thus increases the assembly cohesion, and 2) reactivity between the polymer and the Ca^{2+} ions, the $Ca(OH)_2$ crystals, and the surfaces of silicate phases, in particular the C-S-H gel. Sinclair and Groves (3) have shown that the reaction between polyacrylamide and cement results in amorphous, calcium-rich, polymeric-containing phases. Sakai and Sugita (4) have suggested that spheroidal particles of polymer are localized along the interface between anhydrous cement grains and hydration products. For the pore distribution, Ohama (1) and Fu and Chung (5) have found that polymer-modified cement (PMC) contains less large (>0.2 μm) pores than polymer-free cement (PFC) but more small (<75 nm) pores. The present study compares the microstructures, hydration rate, and porosity of a PMC and a PFC.

Communicated by D. Sorrentino.

[1]To whom correspondence should be addressed.

Experimental

Materials

The acrylic polymer emulsion was made by mixing water with 50% butylacrylate (BA), 48.5% methylmethacrylate (MMA), and 1.5% methylmethacrylic acid (MAA), with addition of 0.36% of anionic stabilizer and 3% of nonionic stabilizer. The mean size of polymer particles was 180 nm. The pH of the medium was 9.65. Viscosity of the slurry was 64 cP for a dry-matter content of 47%.

The cement was a Portland cement (CPA-CEM I 52.5 PMES CP, Lafarge) with Bogue composition of 66.0 of C_3S, 18.3% of C_2S, 4.3% of C_3A, 6.3% of C_4AF, and 5.0% of gypsum. The water-to-cement ratio was 0.33 for both the PMC and the PFC. For the PMC, the polymer-to-cement ratio was 0.1. The cure was of 28 days at 23°C, in 50% relative humidity.

Characterization

Scanning electron microscopy (SEM) was done using a field-emission microscope (LEO 982) that does not require any special preparation of the sample. X-ray diffraction (XRD) was done using a Bragg-Brentano chamber mounted on a Philips PW 1729 generator (Cu Kα radiation). Thermal analyses (differential thermal analyis-thermogravimetric [DTA-TG]) were done using a SDT 2960 (TA-Instruments) simultaneous apparatus with a platinum crucible. Heating rate was $5°C \cdot min^{-1}$ from room temperature to 750°C. Mercury porosimetry was done using Autopore-II 9215 (Micromeritics). For PFC and PMC, experiments were carried out either after cure or after heat treatment at 390°C. Thermal analyses showed that a temperature of 390°C is superior to the temperature of polymer pyrolysis but inferior to the temperature of portlandite decomposition. Adsorption isotherms of water vapor were registered using an automatic microgravimeter (AGLAE) (6). This apparatus allows the determination of BET specific area and pore width distribution (7) of small pores (between 1 and 10 nm), which complements mercury porosimetry whose inferior limit is of about 0.2 nm.

Results and Discussion

Microscopy

In cured PMC, SEM observations show the presence of spheroidal globules with mean diameter of 200 nm. One fraction of globules is homogeneously incorporated at the inside of hydrates; the rest is segregated to form beads around nonhydrated cement grains. The size of the globules is very close to that of the polymer particles (180 nm), which supports the assimilation of the globules to the particles. Figure 1 illustrates a typical shell structure (going from the exterior toward the center of the grain) of 1) granule-containing hydrates, 2) granule beads, and 3) anhydrous cement grain. This observation extends the model of Ohama (1) by showing that a fraction of the polymer is trapped at the inside of hydration products and the rest is segregated onto the surface of still-anhydrous cement grains. This implies that the polymer has three effects: 1) it partially obstructs the fine pore network inside of hydrates;

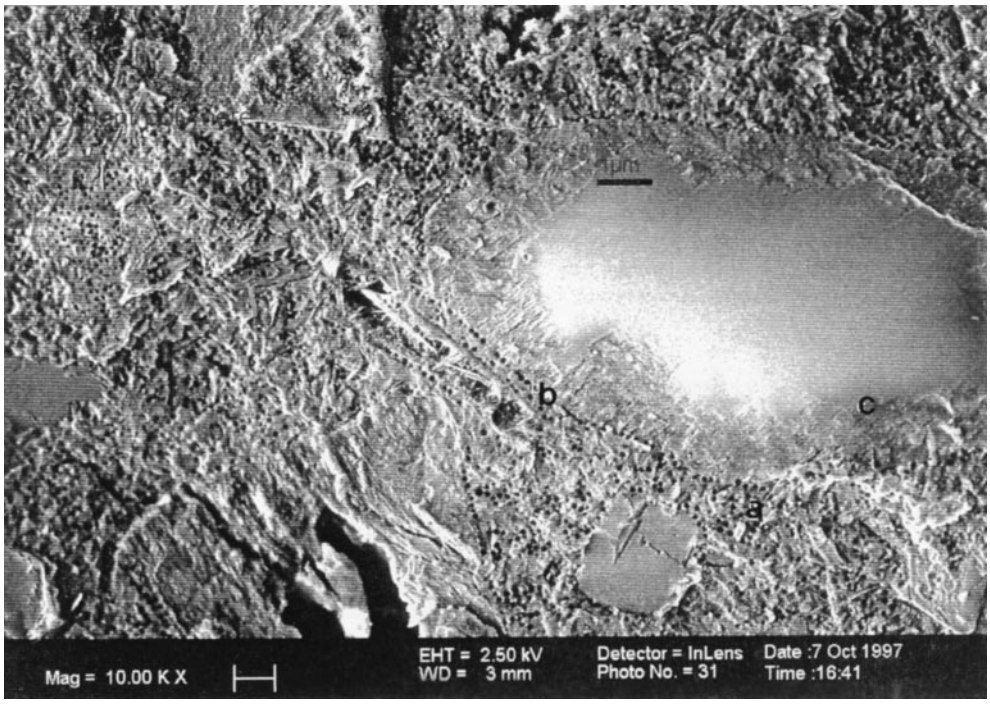

FIG. 1.
SEM micrograph of the PMC, showing the shell structure of globule-containing hydrates (zone a), globule beads (boundary b), and still-anhydrous cement grain (zone c) (fracture surface).

2) it fills the large pores; and 3) it forms membranes that encapsulate the cement grains. The effects combine to decrease permeability and hydration rate.

Quantitative image analysis performed on polished surfaces (Fig. 2) allowed us to compare the volume fraction of anhydrous cement in the PFC and PMC.

If N_X is the number of points located at the inside of phase X and N_0 the total number of points, then V_X is the volume fraction of phase X: $V_X = N_X/N_0$.

For every sample, we scanned two areas of $380 \times 506\ \mu m^2$. The results were of about 25% and 50% of anhydrous cement in the PFC and PMC, respectively, which indicates that the polymer strongly decreases the hydration rate.

X-ray diffraction

XRD experiments were conducted on cured PFC and PMC. The XRD patterns (not presented here) show more anhydrous residues (in particular of C_3S and C_2S) and less portlandite in the PMC than in the PFC, which confirms the retardant effect of the polymer.

Thermal analyses

Figures 3 and 4 show the DTA-TG curves of cured PFC and PMC. For the PFC, our results

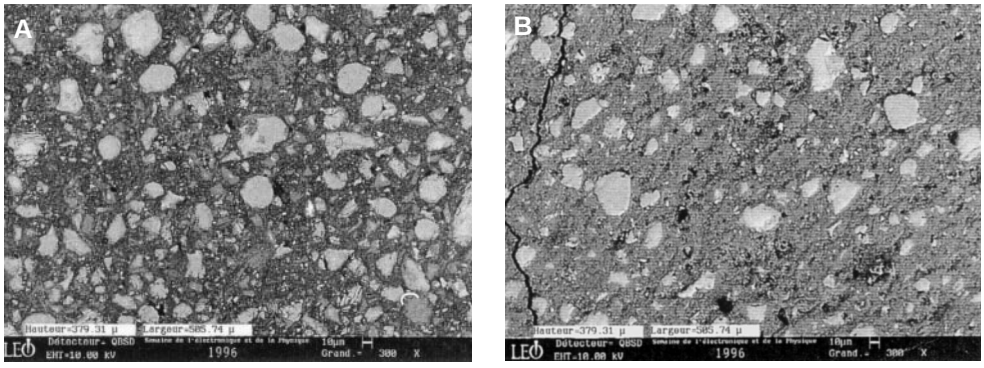

FIG. 2.
SEM micrographs of hydrated pastes cured for 28 days. (A) PFC and (B) PMC (polished surfaces).

agree with those of Baroghel-Bouny (8). From about 70°C to 200°C, the endothermal phenomena correspond to the vaporization of free water and decomposition of C-S-H and hydrated aluminates. The endothermic peak at 435°C is due to the decomposition of portlandite, as confirmed by XRD data (not presented here) on samples quenched from two temperatures, one just inferior and the other just superior to the peak temperature. The weak signal at about 670°C is related to the decarbonatation of $CaCO_3$. For the PMC, we observe two supplementary exothermic peaks at 280°C and 325°C, which are due to the polymer pyrolysis. For the decomposition of portlandite, the weight loss between 390°C and 450°C is 5.2% for the PFC but it is 3.4% only for the PMC, which confirms that the polymer slows down the hydration rate and thus the portlandite formation.

Figure 5 shows the relative content of portlandite in materials cured at 7, 14, 21, and 28

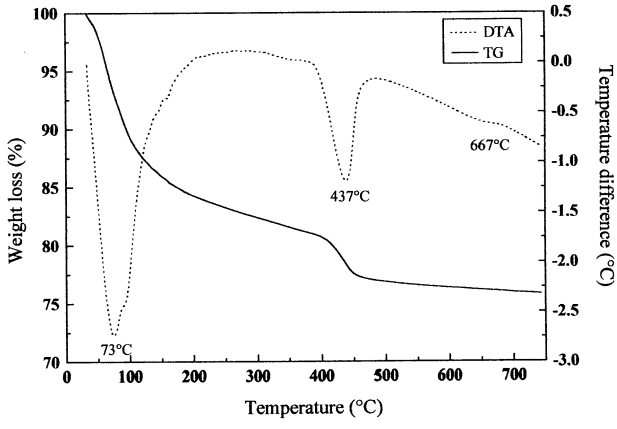

FIG. 3.
DTA-TG curves for a PFC cured for 28 days at 23°C.

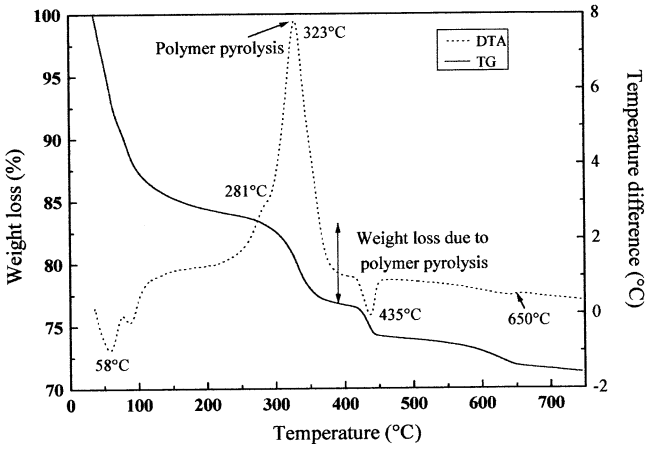

FIG. 4.
DTA-TG curves for a PMC cured for 28 days at 23°C.

days, the data being derived from the integrated area of the portlandite TG peak at 435°C. The lower quantity of portlandite in the PMC is confirmed.

Porosimetry

For mercury porosimetry, Figures 6 and 7 show the pore width distributions in PFC and PMC, after cure and after heat treatment at 390°C.

After cure, PFC and PMC exhibit similar porosity (23–24%), but the PMC has a much larger surface area (24.25 $m^2 \cdot g^{-1}$) than the PFC (15.40 $m^2 \cdot g^{-1}$), which means its pores are smaller. In the PFC, there is a peak in the pore width distribution at about 0.1 μm,

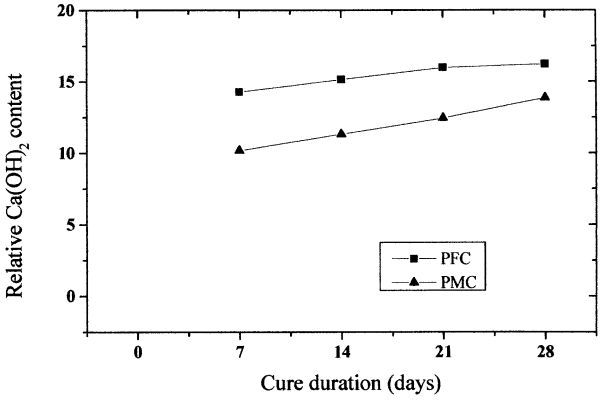

FIG. 5.
Relative content of portlandite vs. cure duration (at 23°C).

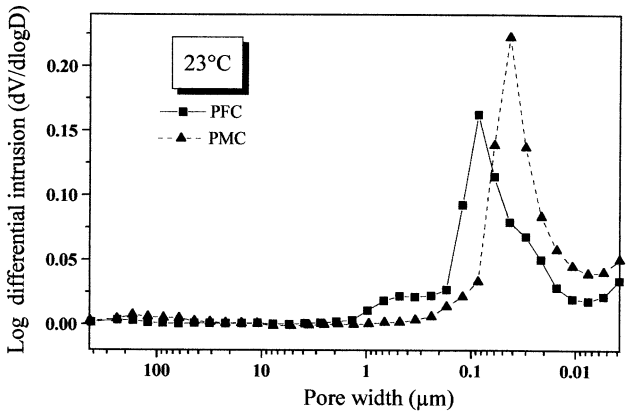

FIG. 6.
Pore width distribution (mercury intrusion) in PFC and PMC cured at 23°C.

characteristic of gel porosity, and a diffuse massif between 0.2 and 0.7 μm, characteristic of capillary porosity and known to be very dependent on the water-to-cement ratio (7). In the PMC, the peak that is characteristic of gel porosity is displaced down to 0.05 μm and the capillary porosity is now entirely below 0.2 μm. The porosity in the PMC is finer than that in the PFC, which indicates that water permeation is reduced.

After heat treatment at 390°C, the PFC porosity is still of about 23–24%, but the PMC porosity has dramatically increased (33.75% instead of 24% after cure). This is due to the pyrolysis of polymer. The pores between 0.2 and 2 μm are "regenerated" and the capillary-pore peak is rather wide.

For porosimetry using AGLAE (pores below 5 nm), Figure 8 shows that there is no

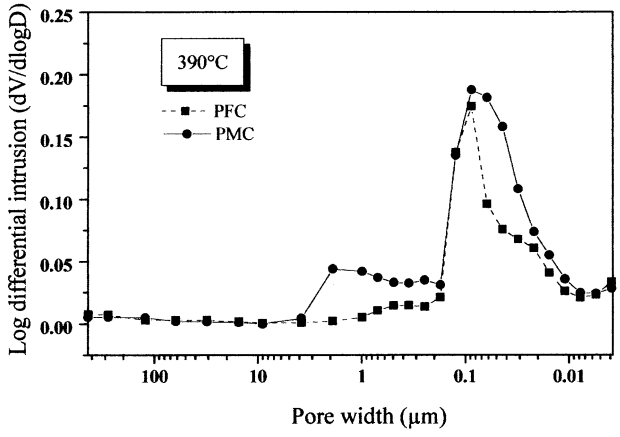

FIG. 7.
Pore width distribution (mercury intrusion) in PFC and PMC heat treated at 390°C.

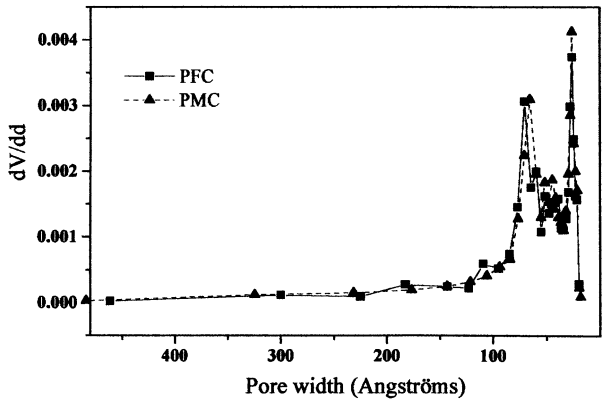

FIG. 8.
Pore width distribution (using AGLAE) in PFC and PMC cured at 23°C.

noticeable difference between the PMC and the PFC, which means the size of the polymer particles (200 nm) is too large to affect the fine porosity significantly.

Conclusions

SEM observations show that the PMC microstructure is characterized by a shell configuration of polymer-containing hydrates, polymer granule beads, and nonhydrated cement grain. The retardant effect of the polymer is marked, which can be due to the polymer membrane that encapsulates the cement grains. In cured pastes, the porous volumes are similar in PFC and PMC, although the presence of polymer shifts the pore width distribution toward smaller values. After heat treatment, the polymer is pyrolized, which results in an increase in porosity of about 10%.

Acknowledgments

The authors gratefully acknowledge D. Sant, who carried out most of the materials preparation, P. Landouar, who allowed us to use the LEO field-emission microscope, and J-P. Guilbaud and P. Vié, who allowed us to use AGLAE.

References

1. Y. Ohama, ACI Mater. J. 84-M45, 511 (1987).
2. S. Chandra and P. Flodin, Am. Concr. Inst. 119, 263 (1989).
3. W. Sinclair and G.W. Groves, J. Mater. Sci. 20, 2846 (1985).
4. E. Sakai and J. Sugita, Cem. Concr. Res. 25, 127 (1995).
5. X. Fu and D.D.L. Chung, Cem. Concr. Res. 26, 985 (1996).
6. A. Raoof, Thesis, Université de Marne la Vallée, France, 1997 (in French).
7. O. Rozenbaum, DEA, Université d'Orléans, France, 1995 (in French).
8. V. Baroghel-Bouny, Caractérisation des pâtes de ciment et de bétons. Méthodes, Analyse, Interprétations, LCPC, Paris, France, 1994 (in French).